BOREAL ENVIRONMENT RESEARCH 13: 433–443
ISSN 1239-6095 (print) ISSN 1797-2469 (online)

Helsinki 31 October 2008

Boreal forest leaf area index from optical satellite images: model simulations and empirical analyses using data from central Finland

Pauline Stenberg[1)], Miina Rautiainen[1)4)], Terhikki Manninen[2)], Pekka Voipio[3)] and Matti Mõttus[1)4)]

[1)] *Department of Forest Resource Management, P.O. Box 27, FI-00014 University of Helsinki, Finland (e-mail: pauline.stenberg@helsinki.fi)*
[2)] *Finnish Meteorological Institute, Earth Observation, P.O. Box 503, FI-00101 Helsinki, Finland*
[3)] *Finnish Forest Research Institute, Suonenjoki Research Unit, Juntintie 154, FI-77600 Suonenjoki, Finland*
[4)] *Tartu Observatory, 61602 Tõravere, Estonia*

Received 12 Oct. 2007, accepted 21 Jan. 2008 (Editor in charge of this article: Jaana Bäck)

Stenberg, P., Rautiainen, M., Manninen, T., Voipio, P. & Mõttus, M. 2008: Boreal forest leaf area index from optical satellite images: model simulations and empirical analyses using data from central Finland. *Boreal Env. Res.* 13: 433–443.

A key variable controlling the global carbon, water and energy cycles is the leaf area index (LAI), which thus has an important role in current biosphere-atmosphere research. Several international networks promote the development of remote sensing techniques for global assessment of LAI. We present results from the VALERI (VAlidation of Land European Remote sensing Instruments) network's test site at Hirsikangas in central Finland which represents one of the very few boreal forests in the global networks. In this study, three years of LAI data from Hirsikangas together with medium-resolution satellite images (SPOT HRVIR, Landsat 5 TM and IRS) over the site were used (1) to study the relationships between LAI and different spectral vegetation indices (SVIs), and (2) to test the performance of a physically-based forest reflectance model (PARAS). Simulations with PARAS showed good agreement with empirical data. Results indicated that inclusion of the SWIR band improves the performance of SVIs used for LAI estimation in the boreal forests.

Introduction

The leaf area index (LAI) of plant canopies is one of the key variables controlling ecosystem energy, water and gas exchanges and thus has an important role in current global biosphere-atmosphere research (Sellers *et al*. 1997). It is also closely linked to the spectral reflectance (bidirectional reflectance factor, BRF) of plant canopies in the shortwave solar radiation range (Myneni *et al*. 1997) and has a major impact on the surface albedo, which is one of the Essential Climate Variables (ECV) needed as input for climate change modelling as defined in the Implementation Plan for the Global Observing System for Climate in Support of the UNFCCC (URL: http://unfccc.int/2860.php). Assessment of biophysical vegetation parameters over large regional scales is only possible using remote sensing techniques. The retrieval of LAI from optical satellite images

has been considered a feasible mission that has attracted wide research interest. The physical relationships between canopy BRF and LAI form the basis of retrieval algorithms used in current earth observation programs (e.g. MODIS, CYCLOPES, GLOBCARBON products) for mapping LAI at global scales.

Several international networks promote global and regional LAI mapping, product validation and related methodological development (Morisette *et al*. 2006). One of the networks is VALERI (Validation of Land European Satellite Remote Sensing Instruments, URL: http://www.avignon.inra.fr/valeri/). The objectives of the VALERI network are to provide high spatial resolution maps of biophysical variables, such as LAI and the fractions of absorbed photosynthetically active radiation (f_{PAR}) and vegetation cover (f_{cover}), and to validate these products with ground-based measurements. For accomplishing these goals, the VALERI network offers a methodological framework designed for the derivation of high spatial resolution maps, instrumentation for ground measurements and processing, a network of sites distributed over the Earth's surface and a database of processed and available high spatial resolution maps. Two of the VALERI network test sites, Hirsikangas and Rovaniemi, are located in Finland and represent the only European boreal forests of the network.

Ecologically, the boreal zone has a considerable influence on global carbon, water and energy cycles. Northern hemisphere boreal forests form the largest unbroken, circumpolar forest zone in the world. These forests are dominated by coniferous tree species which typically have a clumped canopy structure in combination with a low tree density and abundant understory vegetation. These factors cause the BRF and surface albedo of the northern coniferous forests to differ in many respects from that of other biomes. From the perspective of optical remote sensing, specifically the low reflectance of boreal forests and the narrow range of spectral vegetation indices (calculated from satellite images) used to estimate basic biophysical variables often lead to unreliable image interpretation results (Eklundh *et al*. 2001, Rautiainen *et al*. 2003, Stenberg *et al*. 2004, Rautiainen 2005a, Eriksson *et al*. 2006, Heiskanen 2006).

In this paper, we present measurement and modeling results from a VALERI network test site, Hirsikangas, over a three-year period (2003–2005). The relationships between measured LAI and spectral reflectances obtained from medium-resolution satellite images (SPOT HRVIR, Landsat 5 TM and IRS) from succeeding years were studied empirically in using spectral vegetation indices (SVIs) and theoretically using a physically-based forest reflectance parameterization model which has been specifically designed for a boreal environment.

Material and methods

Site description

The first 3 km × 3 km VALERI site in Finland, called Hirsikangas, was established in 2003 and is located in Suonenjoki (62°38´38´´N, 27°00´41´´E) in central Finland. Approximately 90% of the site is forested area dominated by Scots pine (*Pinus sylvestris*), the rest consisting of agricultural fields, peat production area and small water bodies. Understory vegetation in the forested area is composed mainly of dwarf shrubs (*Vaccinium myrtillus* and *Vaccinium vitis-idaea*). Thirty-three plots, called elementary sampling units (ESUs) in the VALERI network, were chosen and established to give a good coverage of the site both spatially and with respect to stand structure and LAI (Fig. 1). The ESUs included 22 Scots pine stands, one birch (*Betula pendula*) stand, one spruce (*Picea abies*) stand, and six mixed stands with spruce and pine and/or birch. In addition, there were 3 ESUs (a sapling stand, a grass field and an agricultural field) that had no leaf area (i.e. LAI = 0) above the height of measurement (1 m), and were not used in the analysis.

LAI measurements

LAI data from Hirsikangas were collected between 7 and 20 August 2003, between 24 June and 22 July 2004, and between 24 May and 22 June 2005. At each ESU, measurements of LAI were made using the LAI-2000 Plant Canopy Analyzer (Li-Cor Inc., Nebraska, USA) in grids

with 12 measurement points marked by sticks. The grid design, chosen according to VALERI standards, was a cross with measurement points placed at 4 m intervals on a south–north transect (6 points) and on a west–east transect (6 points). The geographic coordinates of the centre points of the plots were measured with GPS (Trimble Geo XT). Two LAI-2000 units were used to obtain simultaneous readings below and above the canopy. Above-canopy readings were collected automatically at regular intervals (every 15 s) in an open area close to the plot. Below-canopy measurements of LAI were made at approximately 1 m above the ground (i.e. only trees were included in the field of view).

Three Scots pine plots that were thinned in 2003, before the LAI measurements but after the acquisition of the satellite image (*see* section "Satellite data"), were excluded from the analysis. LAI data from 2003 thus comprised 27 plots. Data from 2004 and 2005 LAI included 25 and 22 of these plots, respectively. The theoretical analysis (i.e. model simulations) done in this study was restricted to 15 pure Scots pine stands measured in 2003 (*see* section "Reflectance simulations"). Because the LAI-2000 instrument measures an "effective LAI" rather than the true hemisurface (half of total) LAI *sensu* Chen and Black (1992), the LAI-2000 estimates are hereafter denoted as LAI_{eff}. The LAI_{eff} of the ESUs measured in 2003 ranged from 0.3 to 4.5, where the highest values ($LAI_{eff} > 3$) were obtained in birch and mixed spruce-birch stands. LAI_{eff} of the ESUs measured in 2004 and in 2005 ranged from 0.1 to 4.4 and from 0.04 to 3.5, respectively. There were no significant changes in LAI_{eff} from 2003 to 2004, whereas in 2005 a few plots had smaller LAI than in previous years (Fig. 2). This was probably due to the early LAI measurement date (late May) at these plots.

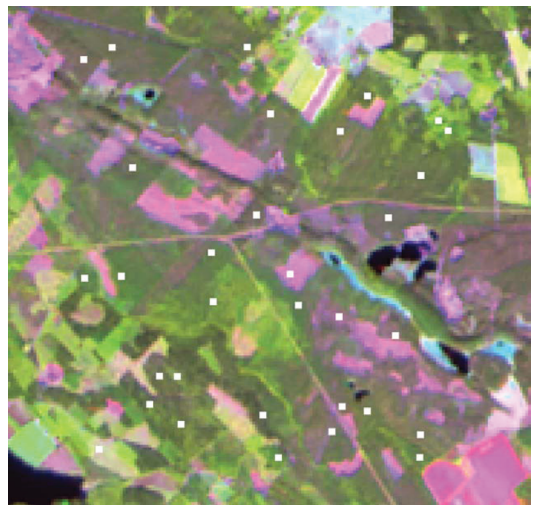

Fig. 1. Sampling design on top of SPOT RGB-composition of channels 2–4 of the Hirsikangas site (62°38´38´´N, 27°00´41´´E).

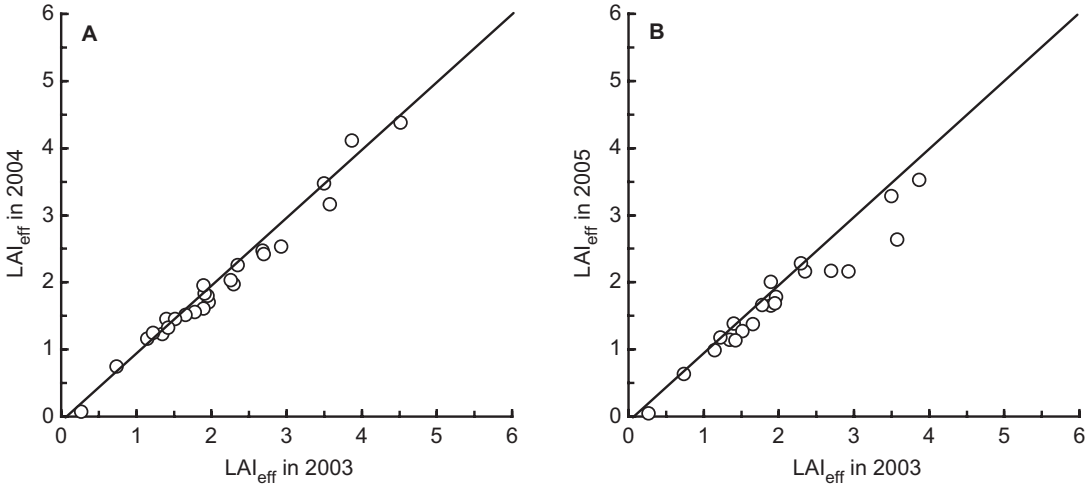

Fig. 2. A comparison of leaf area index of the ESUs in succeeding years. — **A**: LAI_{eff} in 2004 *vs.* LAI_{eff} in 2003. — **B**: LAI_{eff} in 2005 *vs.* LAI_{eff} in 2003.

Satellite data

The satellite data used in this study were from a SPOT HRVIR image (2 August 2003), a Landsat 5 TM image (22 July 2004), and an IRS image (19 June 2005), all provided by the VALERI network. The basic processing of the SPOT image was 2B SpotViewBasic: a precision preprocessing level in which bidirectional geometric corrections are performed using ground control points. A topographic map supplied by the National Land Survey of Finland over the study site was used to extract the four ground control points (two crossroads, a power line crossing and a tip of a lake) that were located within the 3 × 3 km study site. The Hirsikangas area is topographically relatively flat and situated between 975 and 1450 m above sea level. The GPS system used to acquire the ground control points was Trimble Geo XT, with a typical uncertainty of 1 meter when differential correction was applied afterwards. The image was rectified according to the projection commonly used in Finland, the Finnish National Grid (GCS_KKJ, 27South, reference ellipsoid: Hayford). In the 2B product the location accuracy is 30 meters for vertical viewing when maximum elevation differences within the area do not exceed 1250 meters, which can be considered to hold at the study site. The image was georectified to a pixel size of 20 m × 20 m. The image was calibrated into Top-of-Atmosphere (TOA) reflectances with the delivered sensor data. Next, atmospheric correction was done by converting the TOA reflectances into ground reflectances using the SMAC (Simplified Method for Atmospheric Correction, Rahman and Dedieu 1994) procedure, which enables pixelwise corrections. This procedure relies on pre-calculated correction parameters required for each satellite sensor and band. The spectral reflectance of SPOT 3 × 3 pixel windows (representing thus an area of 60 m × 60 m) around the plot centres (ESU midpoints) were averaged to correspond to LAI of the plots, computed as an average over the 12 measurement points of each ESU. The georectification and atmospheric correction of the Landsat 5 TM image was carried out similarly to the SPOT image, except that the pixel size of the georectified image was 30 m × 30 m, instead of 20 m × 20 m. The georectification and atmospheric correction of the IRS image was carried out similarly keeping the pixel size at 20 m × 20 m.

Reflectances in the red, near-infrared (NIR) and shortwave infrared (SWIR) wavelengths were used in the empirical analysis, i.e., SPOT bands 2 (0.61–0.68 μm), 3 (0.79–0.89 μm) and 4 (1.58–1.75 μm), Landsat TM bands 3 (0.63–0.69 μm), 4 (0.76–0.90 μm), and 5 (1.55–1.75 μm), and IRS bands 2 (0.62–0.68 μm), 3 (0.77–0.86 μm) and 4 (1.55–1.70 μm).

Empirical analysis using SVIs

We studied the relationship of three different spectral vegetation indices (SVIs), the normalized difference vegetation index (NDVI), the reduced simple ratio (RSR) (Brown *et al*. 2000), and the infrared simple ratio (ISR) (Fernandes *et al*. 2002) with LAI. The indices are defined as follows:

$$\mathrm{NDVI} = \frac{\rho_{\mathrm{NIR}} - \rho_{\mathrm{RED}}}{\rho_{\mathrm{NIR}} + \rho_{\mathrm{RED}}} \quad (1)$$

$$\mathrm{RSR} = \frac{\rho_{\mathrm{NIR}}}{\rho_{\mathrm{RED}}} \times \frac{\rho_{\mathrm{SWIR\_max}} - \rho_{\mathrm{SWIR}}}{\rho_{\mathrm{SWIR\_max}} - \rho_{\mathrm{SWIR\_min}}} \quad (2)$$

$$\mathrm{ISR} = \frac{\rho_{\mathrm{NIR}}}{\rho_{\mathrm{SWIR}}} \quad (3)$$

where ρ_{RED}, ρ_{NIR} and ρ_{SWIR} are atmospherically corrected reflectances in the red, near-infrared and shortwave infrared spectral bands. We note that the ISR index has also been defined as the ratio of SWIR to NIR (e.g. Fernandes *et al*. 2004), which is equivalent to the moisture stress index (MSI) developed by Rock *et al*. (1986), but here we prefer to define it as in Eq. 3 so that all the compared indices have positive correlation with LAI.

SWIR_min and SWIR_max needed for the RSR index (Eq. 2) were determined from the satellite images as the minimum and maximum values of the SWIR channel for forest pixels only. These were defined as those for which the simple ratio, $\mathrm{SR} = \rho_{\mathrm{NIR}}/\rho_{\mathrm{RED}}$, was greater than or equal to 6. This threshold SR value was chosen, because in the images used the SR distribution density functions of land and forest pixels determined using the CORINE land use map of

25 m resolution (Härmä *et al*. 2004) approximately coincided at values larger or equal to 6. We discovered that masking water areas from the image before the determination of minimum and maximum SWIR reflectances was not crucial. However, it was very important to use only cloud-free image areas, otherwise the maximum value would have been too high.

Table 1. Stand variables for the 15 pure Scots pine plots used in model simulations.

Variable	Min	Max
Tree height (m)	11.3	19.4
Breast height diameter (cm)	10.0	24.9
Stand density (trees ha^{-1})	202	3150

Reflectance simulations

We analyzed the theoretical dependency of forest reflectance at red, near-infrared (NIR) and shortwave infrared (SWIR) wavelengths and of spectral vegetation indices (SVIs) on canopy structure with a physically-based forest reflectance model PARAS (Rautiainen and Stenberg 2005) using as input stand data and LAI from 15 pure Scots pine plots which could be assumed to have similar reflectance properties of foliage and understory. Stand data for the plots (Table 1) were obtained from carrying out relascope sampling at the centre of each plot in July–August 2003. The LAI_{eff} of the plots ranged from 0.7 to 2.4. The simulated reflectance trends were then compared to those obtained from the SPOT HRVIR image obtained at the time of the ground measurements.

The PARAS model is a simple parameterization model where the reflectance of the canopy layer is calculated using the concept of photon recollision probability which allows incorporating clumping at multiple scales. The recollision probability (p) is a spectrally invariant (i.e. wavelength independent) canopy structural parameter, which can be interpreted as the probability by which a photon scattered (reflected or transmitted) from a leaf or needle in the canopy will interact within the canopy again (Smolander and Stenberg 2005). Clumping at different structure levels (e.g. shoot and crown) has a direct influence on p (Mõttus *et al*. 2007).

In the PARAS model, forest BRF is calculated as a sum of the ground and canopy components:

$$\mathrm{BRF} = \mathrm{cgf}(\theta_1)\mathrm{cgf}(\theta_2)\rho_{\mathrm{ground}} + f(\theta_1,\theta_2)i_0(\theta_2)\frac{\omega_L - p\omega_L}{1 - p\omega_L} \quad (4)$$

where θ_1 and θ_2 are the viewing and illumination zenith angles, cgf denotes the canopy gap fraction in the directions of view and illumination (Sun), ρ_{ground} is the BRF of the ground (which may also be expressed as a function of θ_1 and θ_2 depending on the data available), f is the canopy scattering phase function, $i_0(\theta_2)$ is canopy interceptance or the fraction of the incoming radiation interacting with the canopy, and ω_L is needle (or leaf) albedo. The model and its background have been published in Rautiainen and Stenberg (2005).

In the application of the model to Hirsikangas, the input values were determined as follows. The canopy gap fractions and canopy interceptance ($i_0 = 1 - \mathrm{cgf}(\theta_2)$) were obtained directly from the output file of the LAI-2000 measurements conducted at 1 m height at each ESU. Ground reflectance values were based on goniometric measurements made close to the Hirsikangas site (Peltoniemi *et al*. 2005), and needle single scattering albedo values were based on values reported in the literature (Panferov *et al*. 2001) (Table 2). The fraction of radiation scat-

Table 2. Input values for reflectance simulations with the PARAS model.

Input parameter	Red	NIR	SWIR
Needle single scattering albedo, ω_L	0.10	0.70	0.40
Understory BRF, ρ_{ground}	0.10	0.20	0.20
Recollision probability, p	0.65–0.86	0.65–0.86	0.65–0.86

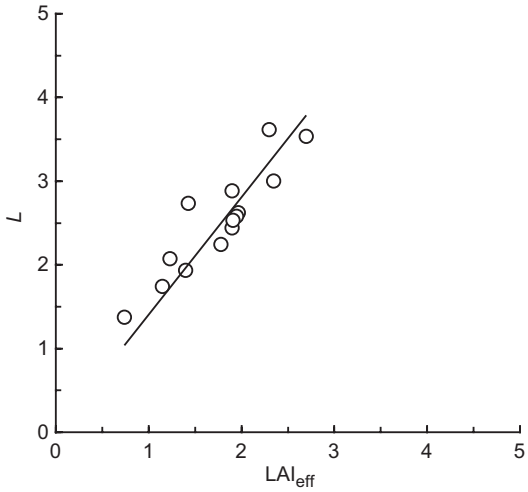

Fig. 3. The relationship of effective LAI (LAI_{eff}) measured with the LAI-2000 instrument and true LAI (L) calculated with Nilson's (1999) algorithm for the pure Scots pine plots used in the reflectance simulations. $L = 1.40LAI_{eff}$, $r^2 = 0.75$.

tered to the view direction (in this case nadir) was approximated using the method of Mõttus and Stenberg (2008).

The photon recollision probability (p) was estimated from the output of the LAI-2000 instrument using a simple analytical formula derived by Stenberg (2007) and tested in Rautiainen *et al*. (2007). The LAI-2000 Plant Canopy Analyzer provides as its output an effective LAI (LAI_{eff}) which, in grouped canopies such as coniferous stands, deviates from the true LAI (L) (e.g. Chen and Cihlar 1995, Stenberg 1996). To calculate p using Stenberg's formula, LAI_{eff} had to be converted to true LAI (L). This was done using the iterative correction algorithm developed by Nilson (1999), which produces an estimate of L from the output of the LAI-2000 instrument and stand inventory data (stand density, mean tree height and crown dimensions) (*see* e.g., Stenberg *et al*. 2003). A fairly linear relationship between L and LAI_{eff} was obtained and L was ca. 40% larger than LAI_{eff} (Fig. 3). The reader should note that in the empirical part of the analyses (i.e. Figs. 2, 4 and 5) we use LAI_{eff}. In the simulation part comprising only the pure Scots pine stands, on the other hand, the true LAI (L) is applied (Figs. 6 and 7).

Results

LAI and empirical forest spectral reflectances and SVIs

To calculate the SVIs (Eqs. 1–3) we used the reflectances obtained from the SPOT (2003), Landsat (2004), and IRS (2005) image 3×3 pixel reflectance windows from their corresponding bands. Comparison of the reflectances obtained for the plots (ESUs) from different images (and years) showed that, in the NIR wavelength, the Landsat (2004) and IRS (2005) reflectances were

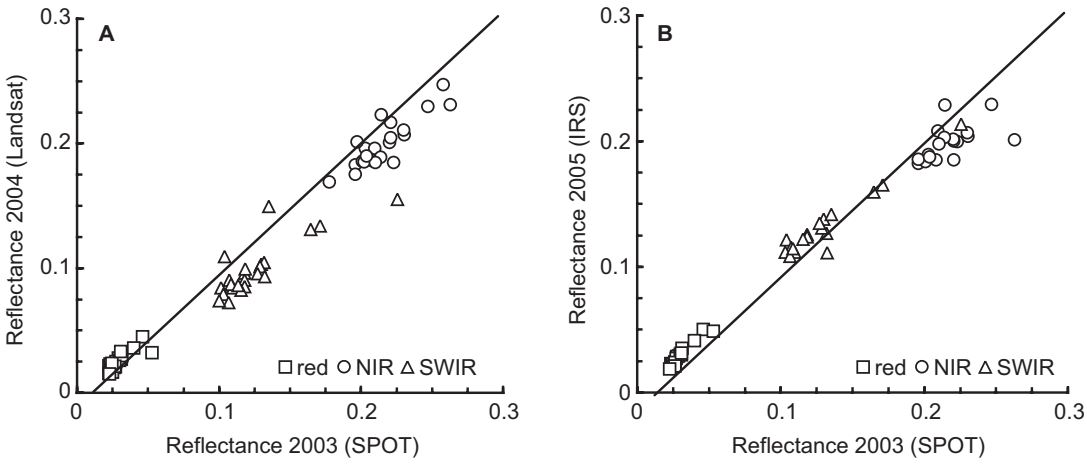

Fig. 4. A comparison of reflectances at red, NIR and SWIR wavelengths for all ESUs. — **A**: SPOT HRVIR (2003) and Landsat 5 TM (2004). — **B**: SPOT HRVIR (2003) and IRS (2005).

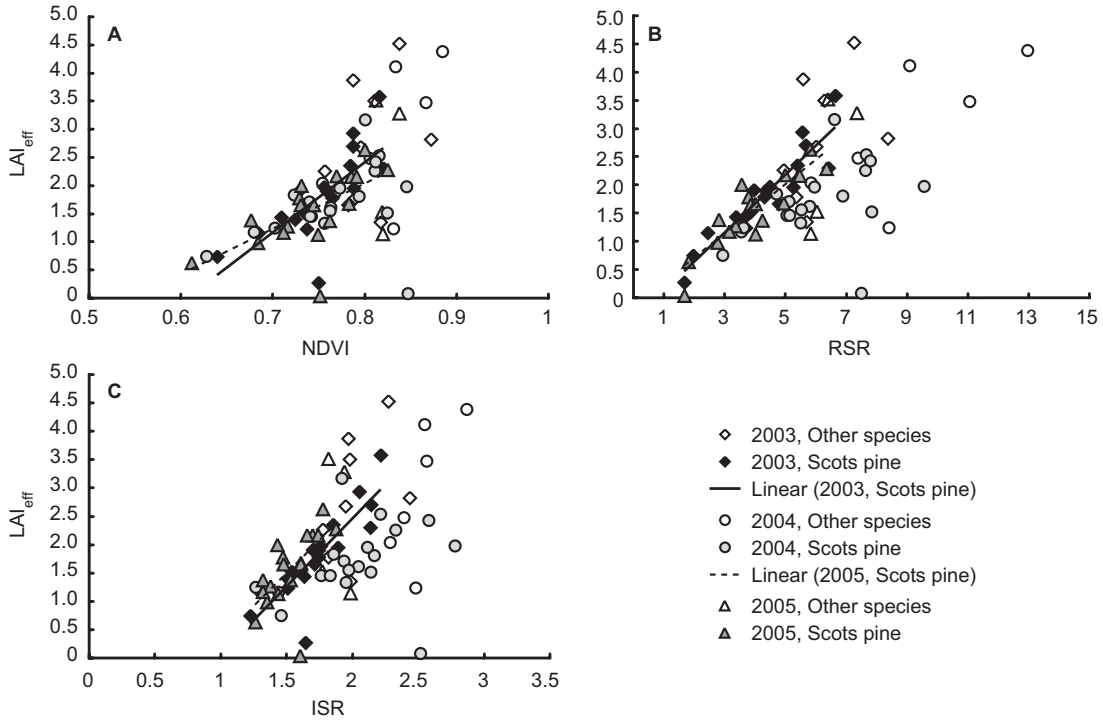

Fig. 5. The relationhip of effective leaf area index (LAI_{eff}) and three vegetation indices for the years 2003–2005. — **A**: NDVI (2003: LAI_{eff} = 12.44NDVI – 7.55, r^2 = 0.53; 2005: LAI_{eff} = 8.06NDVI – 4.42, r^2 = 0.41). — **B**: RSR (2003: LAI_{eff} = 0.52RSR – 0.40, r^2 = 0.85; 2005: LAI_{eff} = 0.43RSR – 0.18, r^2 = 0.79). — **C**: ISR (2003: LAI_{eff} = 2.40ISR – 2.36, r^2 = 0.72; 2005: LAI_{eff} = 2.30ISR – 1.96, r^2 = 0.40).

slightly lower than the SPOT (2003) reflectances but the main difference was observed in the SWIR wavelength, where the Landsat reflectances were clearly lower than the SPOT and IRS reflectances (Fig. 4). A higher than normal SWIR reflectance in the SPOT image may have been explained by the severe drought at the time it was aquired (August 2003). However, this explanation does not apply to the SWIR reflectance in the IRS image (June 2005) which was also higher than that in the Landsat image.

All of the SVIs showed fairly strong positive correlation with the measured leaf area index (LAI_{eff}) in 2003 (SPOT image) and 2005 (IRS image) whereas, for the 2004 LAI and Landsat data, very scattered relationships between LAI_{eff} and the SVIs were obtained (Fig. 5). This was especially true for the indices including the SWIR channel (i.e. RSR and ISR) which, together with the results shown in Fig. 4A, indicates that the atmospheric correction at this channel might have been problematic due to partial thin cloud and haze cover with distinct small cloudlets close to the test site. Of the three SVIs, RSR performed best, followed by ISR, both in terms of correlation and stability between years, i.e. the regressions were quite similar in 2003 and 2005. In contrast, the relationships between LAI and NDVI were quite different in 2003 and 2005. Including all species (i.e. also the few spruce and birch plots) in the regressions reduced the coefficients of determination as compared with those for Scots pine (Fig. 5) by 10% to 20%.The regression parameter values changed by 5% to 15%, except for the slopes of the RSR–LAI relationships, which changed less than 3%.

LAI and simulated forest spectral reflectances and SVIs

Simulations with the PARAS model using the 'true' LAI (L) of 2003 at all the studied wavelengths produced similar trends in reflectance

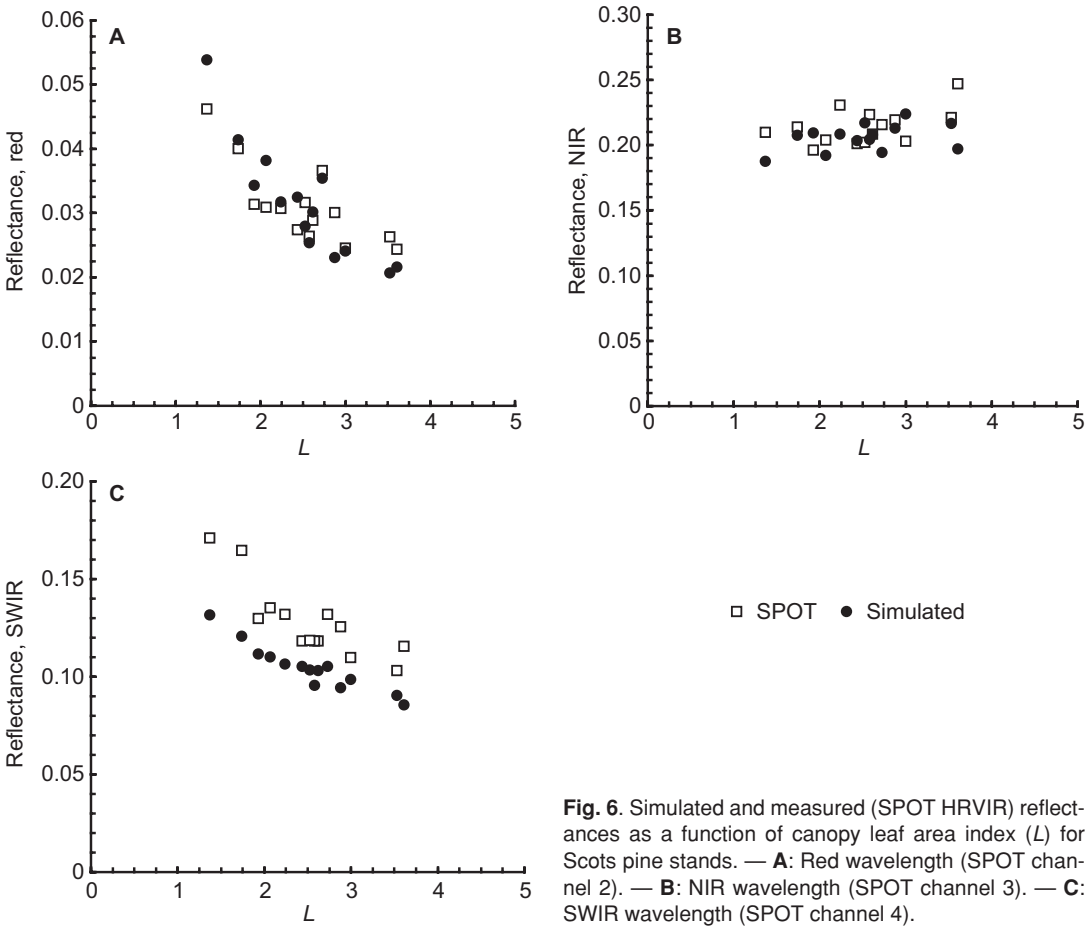

Fig. 6. Simulated and measured (SPOT HRVIR) reflectances as a function of canopy leaf area index (*L*) for Scots pine stands. — **A**: Red wavelength (SPOT channel 2). — **B**: NIR wavelength (SPOT channel 3). — **C**: SWIR wavelength (SPOT channel 4).

with increasing LAI as the measured ones (Fig. 6). In the red and NIR wavelengths, there was also very good agreement between the absolute (simulated and measured) reflectance values, whereas in the SWIR wavelength the simulated reflectance values were somewhat lower than the measured ones. Simulated SVIs confirmed the result from the empirical analysis, namely that among the studied indices, RSR has the most dynamic response to changes in LAI whereas NDVI saturates at medium values of LAI (Fig. 7).

Discussion

As noted in several previous investigations (Brown *et al*. 2000, Stenberg *et al*. 2004, Rautiainen 2005b), inclusion of the SWIR band improves the performance of both SVIs and physically-based forest reflectance models used for LAI estimation in the northern boreal forests (Fig. 5). In these forests, NDVI typically has a narrow range, on one hand due to abundant (green) understory (rather high NDVI even at overstory LAI = 0) and, on the other hand, due to saturation of the index at fairly low values of LAI (Fig. 7). As shown (both theoretically and empirically) in Fig. 6, the reflectance in NIR is almost insensitive to changes in (overstory) LAI, which reduces the dynamics of both NDVI and ISR (Figs. 5 and 7). RSR performed clearly best of the indices but a practical problem with using RSR is how to choose the maximum and minimum reflectances in SWIR (Eq. 2) in an objective manner. On one hand, the minimum and maximum values must be obtained from the image in order to take into account the dynamic range that prevails in the SWIR channel. On the

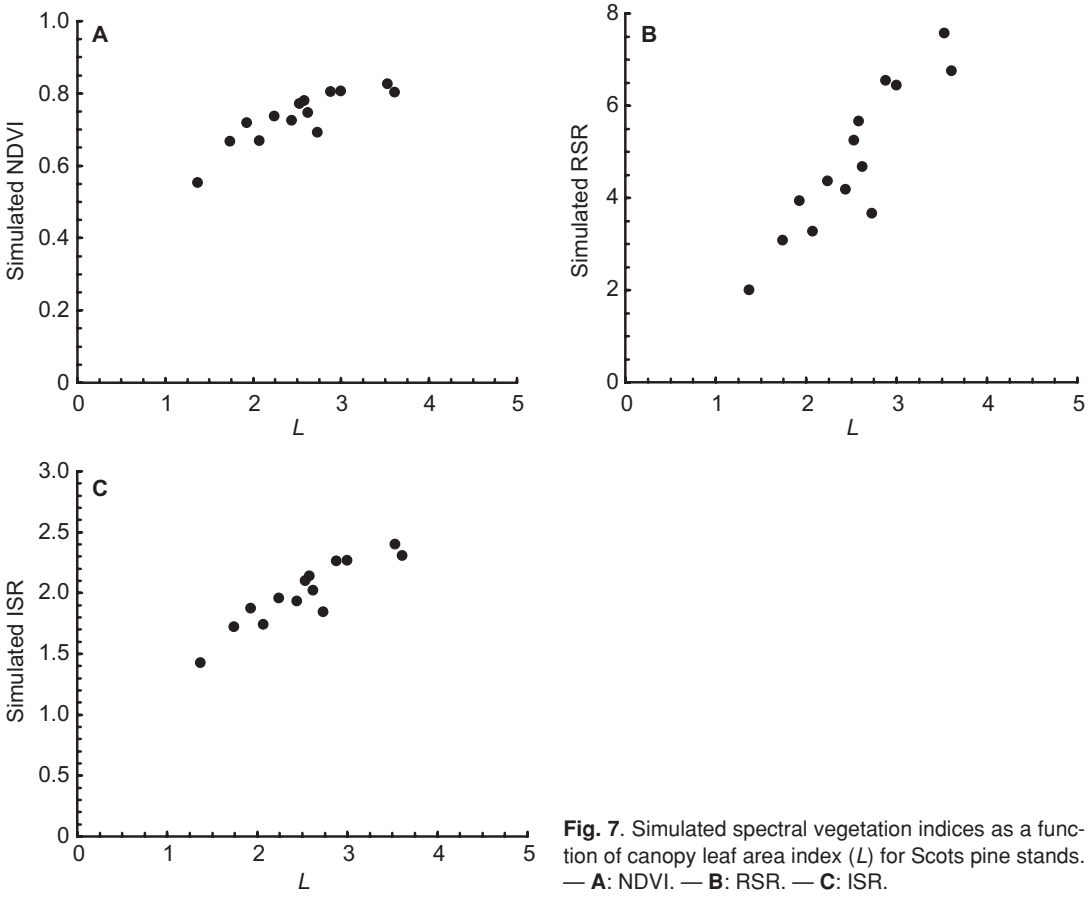

Fig. 7. Simulated spectral vegetation indices as a function of canopy leaf area index (*L*) for Scots pine stands. — **A**: NDVI. — **B**: RSR. — **C**: ISR.

other hand, there must be an operator-independent rule for determining the values. The following method was developed in this paper.

Because the simple ratio, SR, is related to leaf area index, the variation range for the SWIR channel reflectance in a forest can be estimated by taking into account only the pixels for which the SR value exceeds a given threshold value (defined for forest). The threshold value was obtained by comparing the distribution density function of SR values for forest (normalized by the maximum frequency of forested area) to that of all land pixels. The smallest SR value where the forest and land area distribution density functions still coincided (i.e. SR = 6) was chosen to be the threshold value for determination of the SWIR minimum and maximum reflectance values. This guaranteed that only the SWIR minimum and maximum will depend on the image used.

The method worked well and practically the same SR value applied to SPOT, Landsat and IRS images for the three different years and months. However, one has to keep in mind that all the images used were taken during a relatively stable phase of the phenological cycle, after the rapid spring changes. For early summer images, the SR value density distribution would be shifted to smaller values, so that also the threshold value to be used should be smaller. So far the method has been tested only in boreal and sub-arctic forests, where the same threshold was applicable. It is not known whether the same value could be used for other forest types.

We discovered that using different parts of the images for the SWIR variation range determination had only a small effect on the regression-based estimates of LAI (Fig. 5), typically in the order of at most 3% when LAI exceeded 0.5. Both the minimum and maximum SWIR reflect-

ance value of forest typically corresponded to the threshold SR value so that only one condition was needed to determine both ρ_{SWIR_min} and ρ_{SWIR_max}.

To conclude, results from the empirical study strongly encourage the use of SWIR channels in estimating LAI in boreal, conifer-dominated regions. The generally good performance of the PARAS model to reproduce the stand reflectances on the other hand indicates the usefulness of the physically-based approach even when information on all the various parameters that in principle affect stand reflectance is not available. Physically-based, theoretical models have the advantage over empirical models, including spectral vegetation indices (SVIs), that they are less site- and sensor specific. They are also able to separate better the background (soil and understory) reflectance from canopy reflectance, especially since the relative contributions of the ground and tree layer components differ along with sensor and sun angles. A specific advantage of PARAS is its general applicability since it requires relatively few and measurable input parameters. Another advantage is that the dependency of canopy reflectance on LAI is embedded in the spectrally invariant parameter p (the recollision probability) which ensures a consistent behaviour of model simulations at different wavelengths (Panferov *et al*. 2001). Previous simulation runs using the PARAS model have, for example, already shown that a major improvement in simulating canopy reflectance in NIR was achieved by simply accounting for the within-shoot clumping in calculating p (Rautiainen and Stenberg 2005).

For parameterization of PARAS, canopy gap fractions and canopy interceptance (cgf and i_0, Eq. 2) in the viewing and illumination directions can be obtained from, for example, measurements made with the LAI-2000 Plant Canopy Analyzer (or similar devices, including hemispherical photography). The LAI-2000 instrument measures canopy gap fraction in five different zenith angle bands of which the readings of ring 1 (0°–13°) and ring 3 (32°–43°) can be used, for example, in the case of SPOT, Landsat and IRS images in Finland to obtain the viewing and illumination gap fractions. These angles correspond well with the Sun and satellite angle at the moment the image is acquired. Obtaining the input for ground reflectance (ρ_{ground}, first part of the sum in Eq. 4) is both more complicated and measurement intensive, and the interconnected relationship of canopy cover, canopy geometry and abundance of understory vegetation makes calculating the component challenging. Furthermore, it should be recognized, once again, that there exist rather scarce data on the needle single scattering albedo for many conifers due to problems with the (definition and) measurement of narrow and non-flat needles. However, the emerging new laboratory measurements techniques (e.g. supercontinuum laser) will hopefully provide more data in the future. As for the PARAS model development, current goals for improvement are to better account for directional properties of the upwards scattered (i.e. reflected) radiation (Mõttus and Stenberg 2008) and to develop (an addition to) the ground reflectance component to allow simulations for snow-covered forest floors (T. Manninen and P. Stenberg unpubl. data).

Acknowledgements: This study was supported by the University of Helsinki research funds (HARAKKA project) and the Academy of Finland (SPRINTER and COOLFUTURE projects). The satellite images were provided by the VALERI network and the atmospheric correction was carried out at VTT Information Technology.

References

Brown L., Chen J., Leblanc S. & Cihlar J. 2000. A shortwave infrared modification to the simple ratio for LAI retrieval in boreal forests: an image and model analysis. *Remote Sensing of Environment* 71: 16–25.

Chen J.M. & Black T.A. 1992. Defining leaf area index for non-flat leaves. *Plant, Cell and Environment* 15: 421–429.

Chen J.M. & Cihlar J. 1995. Plant canopy gap size analysis theory for improving optical measurements of leaf area index. *Applied Optics* 34: 6211–6222.

Eklundh L., Harrie L. & Kuusk A. 2001. Investigating relationships between Landsat ETM+ sensor data and leaf area index in a boreal conifer forest. *Remote Sensing of Environment* 78: 239–251.

Eriksson H., Eklundh L., Kuusk A. & Nilson T. 2006. Impact of understory vegetation on forest canopy reflectance and remotely sensed LAI estimates. *Remote Sensing of Environment* 103: 408–418.

Fernandes R., Miller J.R., Chen J.M. & Rubinstein I.G. 2004. Evaluating image-based estimates of leaf area index in

boreal conifer stands over a range of scales using high-resolution CASI imagery. *Remote Sensing of Environment* 89: 200–216.

Fernandes R., Leblanc S., Butson C., Latifovic R. & Pavlic G. 2002. Derivation and evaluation of coarse resolution LAI estimates over Canada. In: *Proceedings of Geoscience and Remote Sensing Symposium, 2002*. IGARSS 02.2002 IEEE International Publication, vol. 4, pp. 2097–2099.

Härmä P., Teiniranta R., Törmä M., Repo R., Järvenpää E. & Kallio M. 2004. Production of CORINE2000 land cover data using calibrated LANDSAT 7 ETM satellite image mosaics and digital maps in Finland. In: *Proceedings of the IEEE International Geoscience and Remote Sensing Symposium Anchorage, AK, September 20–24, 2004*, IEEE 4, pp. 2703–2706.

Heiskanen J. 2006. Estimating aboveground tree biomass and leaf area index in a mountain birch forest using ASTER satellite data. *International Journal of Remote Sensing* 27: 1135–1158.

Morisette J., Privette J., Baret F., Myneni R., Nickeson J., Garrigues S., Shabanov N., Fernandes R., Leblanc S., Kalacska M., Sanchez-Azofeifa G., Chubey M., Rivard B., Stenberg P., Rautiainen M., Voipio P., Manninen T., Pilant D., Lewis T., Iiames T., Colombo R., Meroni M., Busetto L., Cohen B., Turner D., Warner E. & Petersen G. 2006. Validation of global moderate resolution LAI products: a framework proposed within the CEOS Land Product Validation subgroup. *IEEE Transactions on Geoscience and Remote Sensing* 44: 1804–1817.

Mõttus M. & Stenberg P. 2008. A simple parameterization of canopy reflectance using photon recollision probability. *Remote Sensing of Environment* 112: 1545–1551.

Mõttus M., Stenberg P. & Rautiainen M. 2007. Photon recollision probability in heterogeneous forest canopies: compatibility with a hybrid GO model. *Journal of Geophysical Research — Atmospheres* 112, D03104, doi: 10.1029/2006JD007445.

Myneni R.B., Ramakrishna R., Nemani R. & Running S. 1997. Estimation of global leaf area index and absorbed par using radiative transfer models. *IEEE Transactions on Geoscience and Remote Sensing* 35: 1380–1393.

Nilson T. 1999. Inversion of gap frequency data in forest stands. *Agricultural and Forest Meteorology* 98–99: 437–448.

Panferov O., Knyazikhin Y., Myneni R., Szarzynski J., Engwald S. & Schnitzler K. 2001. The role of canopy structure in the spectral variation of transmission and absorption of solar radiation in vegetation canopies. *IEEE Transaction on Geoscience and Remote Sensing* 39: 241–253.

Peltoniemi J.I., Kaasalainen S., Näränen J., Rautiainen M., Stenberg P., Smolander H., Smolander S. & Voipio P. 2005. BRDF measurement of understorey vegetation in pine forests: dwarf shrubs, lichen and moss. *Remote Sensing of Environment* 94: 343–354.

Rahman H. & Dedieu G. 1994. SMAC: a simplified method for the atmospheric correction of satellite measurements in the solar spectrum. *International Journal of Remote Sensing* 15: 123–143.

Rautiainen M. 2005a. The spectral signature of coniferous forests: the role of stand structure and leaf area index. *Dissertationes Forestales* 6: 1–54.

Rautiainen M. 2005b. Retrieval of leaf area index for a coniferous forest by inverting a forest reflectance model. *Remote Sensing of Environment* 99: 295–303.

Rautiainen M. & Stenberg P. 2005. Application of photon recollision probability in coniferous canopy reflectance simulations. *Remote Sensing of Environment* 96: 98–107.

Rautiainen M., Stenberg P., Nilson T., Kuusk A. & Smolander H. 2003. Application of a forest reflectance model in estimating leaf area index of Scots pine stands using Landsat 7 ETM reflectance data. *Canadian Journal of Remote Sensing* 29: 314–323.

Rautiainen M., Suomalainen J., Mõttus M., Stenberg P., Voipio P., Peltoniemi J. & Manninen T. 2007. Coupling forest canopy and understory reflectance in the Arctic latitudes of Finland. *Remote Sensing of Environment* 110: 332–343.

Rock B.N., Vogelmann J.E., Williams D.L., Vogelmann A.F. & Hoshizaki T. 1986. Remote detection of forest damage. *Bioscience* 36: 439–445.

Sellers P.J., Dickinson R.E., Randall D.A., Betts A.K., Hall F.G., Berry J.A., Collatz G.J., Denning A.S., Mooney H.A., Nobre C.A., Sato N., Field C.B. & Henderson-Sellers A. 1997. Modeling the exchanges of energy, water, and carbon between continents and the atmosphere. *Science* 275: 502–509.

Smolander S. & Stenberg P. 2005. Simple parameterizations of the radiation budget of uniform broadleaved and coniferous canopies. *Remote Sensing of Environment* 94: 355–363.

Stenberg P. 1996. Correcting LAI-2000 estimates for the clumping of needles in shoots of conifers. *Agricultural and Forest Meteorology* 79: 1–8.

Stenberg P. 2007. Simple analytical formula for calculating average photon recollision probability in vegetation canopies. *Remote Sensing of Environment* 109: 221–224.

Stenberg P., Nilson T., Smolander H. & Voipio P. 2003. Gap fraction based estimation of LAI in Scots pine stands subjected to experimental removal of branches and stems. *Canadian Journal of Remote Sensing* 29: 363–370.

Stenberg P., Rautiainen M., Manninen T., Voipio P. & Smolander H. 2004. Reduced simple ratio better than NDVI for estimating LAI in Finnish pine and spruce stands. *Silva Fennica* 38: 3–14.